# HEAT TRANSFER DURING BOILING ON HEATING SURFACES IN A DISPERSE LAYER OF SOLID PARTICLES: ANALYSIS AND GENERALIZATION OF EXPERIMENTAL DATA

M. I. Berman and Z. R. Gorbis

UDC 536.423.1:66.096.5

An analysis is given and experimental results are generalized for the boiling of water, ethanol, and aqueous solutions at reduced pressures on heating surfaces in a disperse layer of unbound solid particles for limiting (with respect to heat-transfer intensity) conditions.

Earlier [1], it was suggested that the natural motion of vapor and liquid in boiling be used to bring particles of a bed to a mobile state, known as a state of "thermal fluidization" [2].

In the present work, the results of an experimental investigation of this process, some of which were published in [2-5], are generalized. The experimental conditions are given in Table 1.

In the given conditions, the realization of a particular set of hydrodynamic conditions is determined by the relation $\tilde{d}_p$, $\tilde{H}$, $w \equiv Q/r\rho_v s = f(q, p,$ geometry of the apparatus, kind of liquid).

By visual observation and photographic recording of the conditions of motion of the components and phases in the given disperse system and comparing these with experimental heat-transfer data (Figs. 1 and 2), it is possible to establish, in the given conditions, the characteristic values $\tilde{H} = \tilde{H}_{lim}$, $q \equiv q^*$, $w_{s.c} \simeq w(q^*)$, $\tilde{d}_p$ at which change in the disperse-system structure and the heat-transfer laws are observed, and to develop a classification of the conditions of motion of the components and phases during boiling in the given conditions.

According to this classification, shown in Table 2, each of the three experimentally observed structure groups has a specific heat-transfer law. For example, with increase in height of the disperse layer from 0 to $\tilde{H} = \tilde{H}_{lim}$ (conditions 1-3 in Table 2), increase in heat-transfer intensity is observed, while for $\tilde{H} \geq \tilde{H}_{lim}$ (conditions 4-9) heat transfer is self-consistent with respect to $\tilde{H}$ [2, 4]. The heat-transfer intensity when $\tilde{H} \geq \tilde{H}_{lim}$ may exceed by a factor of 2-3 the heat-transfer intensity during boiling in free conditions for the same q, p. Approximate evaluation of the forces acting on a vapor bubble in the conditions $\tilde{H} \leq \tilde{H}_{lim}$ leads to the expression

$$H_{lim} = \sqrt{\sigma/c_1 g(\rho_L - \rho_v) - c_2 g(1-m)(\rho_p - \rho_L)}.$$

In the given conditions $\rho_L \gg \rho_v$, m, $\rho_p \simeq$ idem, according to experimental data, $H_{lim} = (6\text{-}7)\sqrt{\sigma/g\rho_L}$. Because of the small practical value of mechanically unstable conditions of thermal fluidization with $\tilde{H} < \tilde{H}_{lim}$, the subsequent discussion refers mainly to data obtained with $\tilde{H} \geq \tilde{H}_{lim}$. These conditions correspond to structure groups with vapor motion along individual vapor channels (conditions 4-7 in Table 2) and the structure with circulational thermal fluidization of the disperse layer (set of conditions 9 in Table 2). The effect on the heat transfer of pressure, the kind of liquids, the boundary conditions, and the material and thickness of the heating surface is found to be qualitatively analogous to that observed for boiling in the same conditions without a disperse layer of particles (H = 0). This indicates a certain analogy in the occurrence of the two processes. Conditions 4-5a and 7 in Table 2 correspond to boiling curves of the form $\alpha \sim q^{2/3}$ (with decrease in pressure, a weak rise in the power to which q is raised occurs), conditions 4-6b to $\alpha \sim q^{1/2}$ (Fig. 1), and conditions of circulational thermal fluidization (9 in Table 2) to $\alpha \sim q^0$. The effect of particle size on heat-transfer intensity at $q < q^*$ is clear from Fig. 2, according to which the range $\tilde{d}_p = 0.8\text{-}1.3$ is optimal from the point of view of intensifying heat transfer. At $q > q^*$, heat-transfer is self-consistent with respect to $\tilde{d}_p$.

Odessa Technological Institute of the Cooling Industry. Translated from Inzhenerno-Fizicheskii Zhurnal, Vol. 38, No. 1, pp. 5-15, January, 1980. Original article submitted February 27, 1979.

0022-0841/80/3801-0001 $07.50 

TABLE 1. Experimental Conditions

| Heating conditions | Heating surface shape | Material and thickness of heating surface | $R_a$, μm | Liquid | p, bar | Particle mater. | Shape | $d_T$ ($s_{d_T}$), mm |
|---|---|---|---|---|---|---|---|---|
| Direct electrical heating | Horizontal plate, 100 × 15 mm | copper, 0.1 mm | 0,28 | Water | 0,035—1,0 | Glass | Sphere | 0,624(0,027) |
| | | Kh18N10, " | 0,13 | Ethanol | 0,1—1,0 | " | " | 1,33(0,072) |
| | | Nichrome, 0.2 mm | 0,13 | | | " | " | 2,28(0,16) |
| | | | | | | | " | 3,42(0,28) |
| Convective | Horizontal tube, 10 mm diam., L = 620 mm | copper, 1.0-1.5 mm | 0,27 | Water | 0,035—0,7 | alumi-nosili-cate | " | 2,77(0,93) |
| | | | 0,27 | Ethanol | 0,1—1,0 | | | |
| | | Kh18N10, 1.0 mm | | Sol'n of NaCl 0—20% | 0,035—0,5 | Mullite | " | 5,61(0,24) |
| | | | | | | Mullite | " | 9,24(0,43) |
| | | | | | | Cor-undum | Irreg-ular | 0,1 |
| | | | | Sol'n of $C_2H_2O_4$ 20% | 0,35—0,5 | Cor-undum | " | 0,05 |
| | | | | Yeast suspen-sion | 0,035—0,5 | Silica | " | 0,002 |
| " | Horizontal five-row tube bundle F = 0.17 $m^2$ | copper, 1.0 mm | 0,27 | Water | 0,1—0,5 | Glass | Sphere | 2,77(0,93) |
| | | | | Sol'n of NaCl 0—20% | 0,2 | | | |
| | | | | Seawater 11% | 0,2 | | | |

Visual observations indicate that during boiling in conditions of channel formation the fraction of the heating surface covered by a vapor–liquid layer is close to unity and rises with increase in q, tending to unity. The boiling curves are then the upper limits for the boiling curves in conditions 1-3 and 8-9 of Table 2 (Fig. 1).

On the basis of the high heat-transfer intensity (curve 1 in Fig. 1), the small pulsation amplitude $T_w$, and also the stable (without overheating) operation of the thin-walled heating surface at q = const which are observed in conditions of channel formation (conditions 4-7 of Table 2), it may be concluded that under the vapor–liquid layer visually fixed at the heating surface (Table 2) there is a thin nonsteady liquid film. Between this film and the liquid-immersed particles there is a vapor–liquid layer including layer particles in the structure or not including them (in conditions 5 and 6 of Table 2, with removal of the layer). The thermal resistance of the vapor–liquid layer is due to the hydraulic drag on the vapor motion $\Delta p_{h.d}$ (hydrodynamic depression) and may be taken into account in the value of $\Delta T_{h.d}$. In the conditions considered above, $\Delta p_{h.d} \ll p$, and hence $\Delta T_{h.d} \simeq 0$. The heat-transfer law in these conditions is determined to a considerable extent by the thermal resistance of the liquid film at the wall, as in the case of the similar "coalescing-bubble" conditions for free conditions [6].

In conditions of circulational thermal fluidization (9 in Table 2), the heat-transfer intensity is due to the combined effect of heat transfer in the vaporization of the film at the wall and of convective heat transfer to a fluidized disperse layer. Following [6, 7], the mean heat flux for the given conditions is written as the result of summing heat transferred from the heating surface in the vaporization of the liquid microfilm and the heat transferred convectively from the free parts of the surface to those with the microfilm:

$$\bar{q} = \frac{1}{\tau F}\left(\int_0^\tau\int_{F_F}\frac{\lambda_{ef}\Delta T_F}{\delta}dFd\tau + \int_0^\tau\int_{F_{conv}}\alpha_{conv}\Delta T_{conv}dFd\tau\right)$$

$$= \left(c\frac{\bar{\lambda}_{ef}\xi_F}{\bar{\delta}} + \bar{\alpha}_{conv}\xi_{conv}\right)(\bar{T}_w - T_s - \Delta T_{c.d} - \Delta T_{h.d}). \quad (1)$$

The presence in the liquid of a disperse particle layer may affect both components of the total heat flux in Eq. (1), both because of the change in geometric conditions of the occurrence of transfer processes ($\bar{\delta}$, $\bar{\alpha}_{conv}$) and because of the change in effective transfer properties of the disperse system ($\bar{\lambda}_{ef}$) in comparison with the properties of a homogeneous liquid. Consider now the data for end methods of determining the effective

TABLE 2. Classification of Conditions of Motion of Components and Phases in Disperse System on Boiling

| $N_M$ | Experimental conditions | | $\tilde{d}_p$ | State of particle layer | Type of vapor motion | |
|---|---|---|---|---|---|---|
| | | | | | through layer | at surface |
| 1 | Single heating element | $\tilde{H} < \tilde{H}_{lim}$ | >2 | Motionless | Isolated bubbles | |
| 2 | | | 0,2—1,5 | Unstable thermal fluidization | | |
| 3 | | | <0,2 | Suspension | | |
| 4 | | $\tilde{H} > \tilde{H}_{lim}$ | 1—2 | Motionless | a) $q < q^*$ | |
| 5 | | | 0,2—1 | Partial removal from surface by vapor cavities | Periodically appearing vapor channels | vapor — liquid layer of coalescing vapor cavities |
| 6 | | | <0,2 | Complete removal | b) $q > q^*$ Constantly open vapor channels | Practically continuous vapor flow along heating surface |
| 7 | Tube bundle | $\tilde{H} > \tilde{H}_{lim}$ | $\tilde{d}_{Popt} \simeq$ 0.8-1.3 | $w < w_{s.o} = 0.3$ m/sec: motionless particle state, periodically appearing vapor channels | | |
| 8 | | | | $w_{s.o} - w_{s.c} = 1.4$ m/sec: beginning of thermal fluidization of particle layer | | |
| 9 | | | | $w > w_{s.c}$: stable circulational thermal fluidization; at the center of the evaporator, upward motion of vapor—liquid mixture with particles and at the wall, downward motion of dense immersed layer. The vapor passes through the central region as individual bubbles. | | |

characteristics $\bar{\delta}$, $\bar{\lambda}_{ef}$, and $\Delta\bar{T}$ in the limiting case when $\xi_F = 1$, $\xi_{conv} = 0$. Then Eq. (1) takes the form

$$\bar{q} = c \frac{\bar{\lambda}_{ef}}{\bar{\delta}} (\bar{T}_w - T_s - \Delta T_{c.d} - \Delta T_{h.d}). \tag{2}$$

Evaluation of the effective liquid-film thicknesses $\bar{\delta}$ presents the greatest difficulty. A rigorous mathematical approach is practically impossible in this case. Therefore, structural dependences for $\bar{\delta}$ in the given conditions are obtained from an analysis of literature dependences for the thickness of the microfilms forming in the relative motion of a solid wall and vapor (gas) phase in a liquid [8-11]. Despite the difference in organization conditions and the processes in [8-11], it may be concluded that in these cases

$$\delta = \delta(\nu_L, d, \sigma, g\rho_L, w \text{ or } \tau). \tag{3}$$

In conditions of motion along a solid surface by a vapor-bubble meniscus [10, 11], the initial microfilm thickness $\delta_0 \sim \tau^{1/2}$, where $\tau$ is the time from initial bubble formation. In [6], the effective film thickness in bubble-coalescence conditions is taken to be $\bar{\delta} \sim \nu_L^{1/2}\tau^{1/2} = \nu_L^{1/2}(l/w'')^{1/2}$.

One of the differences arising when a disperse particle layer is present is the determination of the quantity d, a linear dimension characterizing the geometric structure of the disperse system in the region at the wall. In conditions when capillary forces have the predominant influence on microfilm formation, which are untypical of the majority of the present experiments (small q, compressed layer grid with small $\tilde{d}_p$), the analysis yields an expression $\bar{\delta} = \bar{\delta}(d)$. For the case of negligibly small capillary forces (large q and $\tilde{d}_p$), $\bar{\delta} = \bar{\delta}(\nu_L, l/w'')$. When capillary, viscous, and inertial forces are commensurate, $\bar{\delta} = \bar{\delta}(\sigma/g\rho_L, d, \nu_L, l/w'')$. From dimensional considerations, taking the most common value 1/2 for the power to which $\nu_L$ is raised, the following three expressions are obtained for the three cases just considered:

$$\bar{\delta} \sim d^{a'}; \quad \bar{\delta} \sim \left(\nu_L \frac{l}{w''}\right)^{1/2}; \quad \bar{\delta} \sim \left(\nu_L \frac{l}{w''}\right)^{1/2} (d/\sqrt{\sigma/g\rho_L})^a. \tag{4}$$

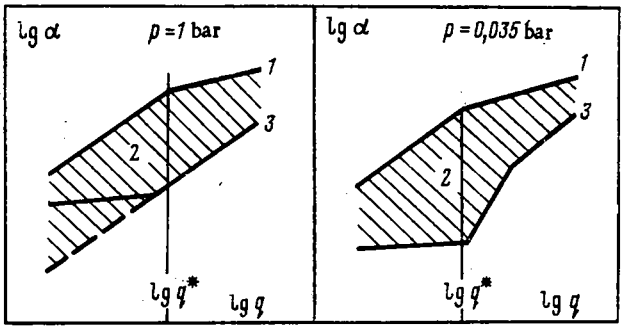


Fig. 1. Boiling curve at a heating surface in a disperse layer of particles: 1) boiling curve with $\tilde{H} \geq \tilde{H}_{lim}$ in conditions of channel formation; 2) boiling-curve region in conditions of thermal fluidization; 3) boiling curves in free conditions (H = 0).

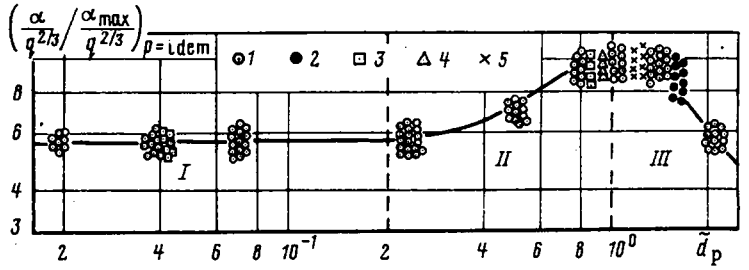


Fig. 2. Effect of particle size on heat transfer during boiling in the conditions $\tilde{H} \geq \tilde{H}_{lim}$: 1) water; 2) ethanol; 3) 20% NaCl; 4) 20% $C_2H_2O_4$; 5) yeast suspension. Surface material: Kh18N10, Nichrome, and copper, p = 0.035-1 bar; I, II) completely and partially removed particle layer; III) motionless layer.

As the defining dimension d for the case of a motionless particle layer (conditions 4 and 7 in Table 2, compressed layer grid), the characteristic dimension of the threshold space in the region at the wall should be chosen to be $d_1 = 2md_p/3(1 - m)$. In conditions of a completely removed layer (6 in Table 2), the maximum layer-removal height $d_2 = [1 - (1 - m_0)/(1 - m_{min})]H_{lim}$ may be chosen as d, where $m_0$ is the porosity of a random covering, $m_{min}$ is the minimum possible porosity. The coicidence of boiling curves for $d_1 = d_2$ confirms the correctness of this choice. In systems with $\tilde{H} \geq \tilde{H}_{lim}$ formed from particles with similar physical properties, the existence of a definite disperse-system structure is determined by the value of $\tilde{d}_p$ (Table 2), which varies over broad limits in the present investigation. For these conditions, in accordance with Fig. 2, the complex $(d\sqrt{\sigma/g\rho_L})^a$ may be written over the whole of the range $\tilde{d}_p \leq 2$ in the form of a continuous function $\varphi'(\tilde{d}_p)$: constant in conditions of a completely removed layer ($\tilde{d}_p \leq 0.2$), decreasing when $0.2 \leq \tilde{d}_p \leq \tilde{d}_{p_{opt}}$, and rising in conditions of a motionless particle layer $\tilde{d}_{p_{opt}} \leq \tilde{d}_p \leq 2$. The minimum $\varphi'$ ($\tilde{d}_p = \tilde{d}_{p_{opt}}$) corresponds to the conditions of maximum heat-transfer intensity in Fig. 2.

In conditions of liquid-film formation, as a result of the coalescence of the menisci of adjacent vapor bubbles ($q < q^*$), $\bar{\delta}$ may be defined as a quantity proportional to the characteristic time interval from the appearance of vapor bubbles to their coalescence $\tau = l/w^n$. Here $l$ is the characteristic distance between active centers [6, 7]. According to [12-14], $l \sim \psi'(\sigma T_s/r\rho_V\Delta T)^k$, where $\psi'$ depends on the material and thickness of the heating surface and the means of heating, while k is 1-1.5 at pressures of the order of atmospheric. Substituting $\bar{\delta} \sim (\nu_L l/w^n)^{1/2}$ into Eq. (2), with $l \sim (\sigma T_s/r\rho_V\Delta T)$ (i.e., k = 1), leads to a structural dependence for the heat transfer from which it follows that $\alpha \sim q^{0.67}p^{0.12}$, which is in good agreement with the present experimental data for heat transfer at pressures close to atmospheric.

For the minimum pressures investigated, the empirical dependence for the heat transfer takes the form $\alpha \sim q^{0.75}p^{0.5}$. Within the framework of the model adopted, this pattern of change in the form of the dependence of $\alpha$ on q and p has a natural explanation: with decrease in pressure, the number of active centers and the

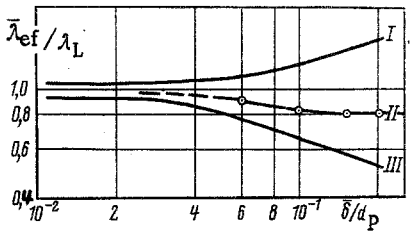


Fig. 3. Effect of particle-material heat conduction on the effective heat conduction of the disperse-system wall region: I, II, III) calculation from Eq. (7) for $\lambda_p \gg \lambda_L$, $\lambda_p \simeq \lambda_L$, $\lambda_p \ll \lambda_L$; the points give the data of electrical modeling for $\lambda_p \simeq \lambda_L$.

distance $l$ between them depend more strongly on $(\sigma T_s/r\rho_v\Delta T)$. For example, change in k as $l$ changes from 1 to 3 leads to change in the approximating structural dependence of the form $\alpha \sim q^n p^s$ from $\alpha \sim q^{0.67}p^{0.12}$ to $\alpha \sim q^{0.8}p^{0.45}$. It may be supposed that the existence of well-founded data for k allows calculational relations for the heat transfer to be obtained within the framework of the model adopted. Since there are no data on $l$ and k for the given case at present, the relation $l \sim \psi'(\sigma T_s/r\rho_v\Delta T)^k$ for thermodynamically similar liquids [15] is taken in the form

$$l \sim \left(\frac{\sigma T_s}{r\rho_v \Delta T}\right) f'(p)\,\psi', \tag{5}$$

which leads to the appearance of the empirical functions f and $\psi$ in the resulting dependence – Eq. (9).

With increase in $\Delta T$, $l$ decreases. However, if at $\Delta T = \Delta T^*(q^*)$ a practically continuous vapor flux arises at the wall, then further change in $l$ with increase in $\Delta T > \Delta T^*$ cannot have any significant effect on the formation of the liquid film at the wall. For these conditions, $l$ is taken to be the characteristic value which it has at the point of change in the hydrodynamic conditions, i.e., $l = l(\Delta T^*)$. Following [15], it may be assumed for thermodynamically similar liquids that $\Delta T^* \sim T_{cr} f''(\tilde{p})$ and

$$l \sim \left(\frac{\sigma T_s}{r\rho_v T_{cr} f''(\tilde{p})}\right) f'(\tilde{p})\,\psi'. \tag{6}$$

Thus, the lack of information on the patterns of distribution and activation of vapor-formation centers at the heating surface means that it is necessary to resort to the concept of approximate thermodynamic similarity in order to close the system of interrelations in the given model. It must be emphasized that generalization of the experimentally obtained information on the heat-transfer laws in the investigation conditions is also possible using only the concept of thermodynamic similarity. However, invoking a model of the detailed process characteristics ($\bar{\delta}$, d, $\bar{\lambda}_{ef}$) permits a more well-founded treatment of the influence of the disperse-layer characteristics on the heat transfer.

Passing now to the analysis of $\bar{\lambda}_{ef}$ – see Eq. (2) – note that in conditions of removal of the layer a homogeneous liquid film remains at the surface, and $\bar{\lambda}_{ef} = \lambda_L$. In the case of a motionless disperse layer, there is a liquid microfilm with particles partially immersed in it at the wall. Particles leaving the surface microfilm enter the vapor–liquid layer. Preliminary estimates of $\bar{\delta}$ from experimental heat-transfer data indicate that, for the investigated layers of motionless particles (Table 2), $\bar{\delta}$ does not exceed $0.2d_p$, and the larger part of the surface of the particle layer at the wall is then found to lie in the region of intense vapor–liquid-mixture motion, the temperature of which is close to $T_s$. Analysis of the quasisteady heat-transfer process in a representative cell of the layer at the wall was carried out in [3] under the assumption that the temperature of the external film surface and of the particles escaping from it is $T_s$. Then heat transfer occurs in the direction normal to the heating surface, and heat transfer radially over the film may be neglected, while for $\bar{\delta}/d_p \leq 0.2$

$$\frac{\bar{\lambda}_{ef}}{\lambda_L} = 1 + \gamma\left[\left(\frac{\bar{\delta}}{d_p}\right) - \left(\frac{\bar{\delta}}{d_p}\right)^2\right], \tag{7}$$

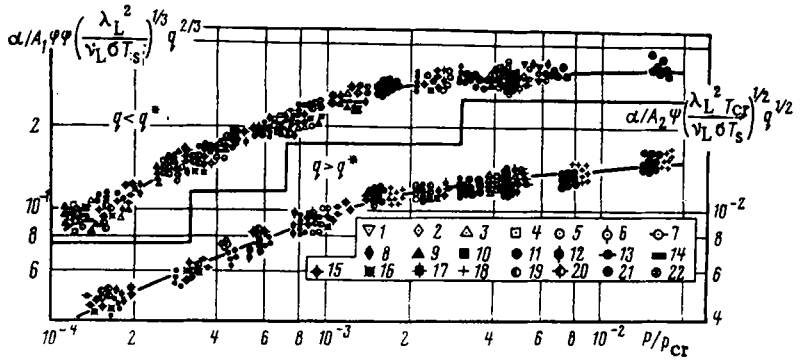


Fig. 4. Generalization of experimental data on heat transfer during boiling on heating surfaces in a disperse layer of solid particles with $\tilde{H} \geq \tilde{H}_{lim}$. The continuous curves correspond to calculation from Eqs. (9)-(11). The experimental points are as follows. For water, q = const: 1, 2) corundum, $d_p$ = 0.05, 0.1 mm; 3, 4, 5, 7) glass, $d_p$ = 0.62, 1.33, 2.28, 3.42 mm; 6) aluminosilicate, $d_p$ = 2.77 mm. For water, convective heating (c.h.), copper, Kh18N10: 8) corundum, $d_p$ = 0.1 mm; 9, 10, 11, 13) glass, $d_p$ = 2.77 mm; 12) aluminosilicate, $d_p$ = 2.77 mm; 14) mullite, $d_p$ = 5.6 mm. For NaCl solution, c.h., copper, glass, $d_p$ = 2.28 mm: 15) 20% NaCl; 16) 10% NaCl; 19) 5% NaCl. For $C_2H_2O_4$ solution (20%), c.h., Kh18N105: 20) glass, $d_p$ = 2.28 mm. For suspension, c.h., copper: 17) aluminosilicate, $d_p$ = 2.77 mm. For ethanol, c.h., copper: 18) glass, $d_p$ = 2.28 mm. For ethanol, c.h., Kh18N10: 21) glass, $d_p$ = 2.28 mm; 22) corundum, $d_p$ = 0.1 mm.

where $\gamma = \pi$ when $\lambda_p \gg \lambda_L$ and $\gamma = -\pi$ when $\lambda_p \ll \lambda_L$ (Fig. 3). This assumes the result of electrical modeling that distortion of the temperature field in the film is observed only in the vicinity of the point at which the particles touch a surface of radius $r_\delta = [d_p^2/4 - (d_p/2 - \bar{\delta})^2]^{1/2}$. For the present case ($\lambda_p \simeq \lambda_L$), electrical modeling of the heat transfer in a representative cell was carried out on an ÉGDA-9/60 electrical integrator. In contrast to [3], heat transfer was modeled in an axisymmetric volume cell. The electrical-modeling data are approximated to Eq. (7) with $\gamma = -1.4$ (Fig. 3). It follows from Fig. 3 that for the given conditions ($\lambda_p \simeq \lambda_L$, $\bar{\delta} < 0$, $2d_p$), the deviation of $\bar{\lambda}_{ef}$ from $\lambda_L$ is less than 20%. Therefore, $\lambda_{ef} = \lambda_L$ is assumed below in generalizing the experimental data.

Good agreement is found if, taking Eq. (7) into account, the present experimental data for a compound glass-particle layer ($\lambda_p \simeq \lambda_L$, $\tilde{d}_p = 0.2$) with $\alpha \sim q^0$ are compared with the data of [16] on boiling in a layer of Monel particles ($\lambda_p \gg \lambda_L$). This may be taken as confirmation that the heat-transfer model adopted is adequate and Eq. (7) is sufficiently accurate.

According to Eqs. (1) and (2), $\Delta\bar{T} = \bar{T}_w - T_s - \Delta T_{c.d} - \Delta T_{h.d}$ In conditions of channel formation, the hydraulic drag of the vapor–liquid at the wall and the vapor channels $\Delta p_{h.d}$ is considerably less than the pressure above the vaporization meniscus p. In this case, $\Delta T_{h.d}$ may be neglected in calculating $\Delta T$. This conclusion is in good agreement with experimental data on the self-consistency of $\alpha$ with respect to $\tilde{H}$ for $\tilde{H} \geq \tilde{H}_{lim}$ [2].

On the basis of the given analysis, in accordance with Eqs. (2)-(7), structural expressions may be obtained for determining the heat-transfer coefficient for the following conditions:

1) when capillary forces have the predominant effect on $\bar{\delta}$, i.e., when particles of small dimension are motionless over the whole bulk of the layer (these conditions are characteristic of [16], for example, and for a whole series of the present experiments with compressed small particles),

$$\alpha = A\bar{\lambda}_{ef}\left[\frac{3(1-m)}{2md_p}\right]^{a'}; \quad (8)$$

2) when capillary, viscous, and inertial forces are comparable (conditions 4-6a and 7 in Table 2) with $q < q^*$,

$$\alpha = A_1 \psi \varphi f_1 \left( \frac{\lambda_L^2}{\nu_L \sigma T_s} \right)^{1/3} q^{2/3}; \tag{9}$$

3) for conditions in which capillary forces are negligible (conditions 4-6b in Table 2) with $q > q^*$,

$$\alpha = A_2 \psi f_2 \left( \frac{\lambda_L^2 T_{cr}}{\nu_L \sigma T_s} \right)^{1/2} q^{1/2} \tag{10}$$

The boundary value $q \equiv q^*$ separating these two sets of conditions is determined by equating $\alpha$ in Eqs. (9) and (10):

$$q^* = \left( \frac{\lambda_L^2 T_{cr}^3}{\nu_L \sigma T_s} \right) \left( \frac{A_2 f_2}{A_1 f_1 \psi} \right)^6.$$

Here $\psi$, $\varphi$, and f are corresponding power functions of the parameters $\psi'$, $\varphi'$, f', and f'' introduced earlier and reflect the influence of the heating-surface characteristics, the relative layer-particle size $\tilde{d}_p$, and the relative pressure $\tilde{p}$. The values of $A_1$ and $A_2$ and the explicit form of the functions $f_1$, $f_2$, $\varphi$, and $\psi$ are found by comparing Eqs. (9) and (10) with experimental data. The value of $\psi$ determined from the experimental data for copper and stainless-steel surfaces also depends on the relative pressure in the range $\tilde{p} \leq 10^{-3}$. The effect of the surface on the heat-assimilation coefficient $\varepsilon_w$ is taken into account for the experimentally observed self-consistency conditions for $\alpha$ with respect to the heating-surface wall thickness $\delta_w$. In determining the form of $\psi$, by analogy with [8, 17], it is assumed that $\alpha$ is related to $\varepsilon_w$ by a smooth dependence $\alpha \sim \varepsilon_w^{\varkappa}$, where the constant $\varkappa > 0$ for thick walls $\delta_w > \delta_{w\,lim}$, for which $\alpha$ is self-consistent with respect to $\delta_w$, and $\varkappa = 0$ when $\delta_w \ll \delta_{w\,lim}$. The expressions for estimating A, $\varphi$, $\psi$, and f determined from approximately 600 experimental values of $\alpha$ take the form

$$f_1 = 0{,}34 - \frac{1{,}54}{10^4 \tilde{p} + 5}; \quad f_2 = 0.015 - \frac{0{,}098}{10^4 \tilde{p} + 8};$$
$$\varphi = 0.79 + 0.24 \sin (2{,}82 \tilde{d}_p - 1{,}55); \tag{11}$$
$$\psi = 1 + 0.5 (\tilde{\varepsilon}_w^{\varkappa} - 1) [1 - \mathrm{th} (3{,}5 \cdot 10^3 \tilde{p} + 1{,}58)];$$

$A_1 = 0.62$, $A_2 = 0.45$ for a wall of thickness of 0.1-0.2 mm and q = const; $A_1 = A_2 = 1$, $\varkappa = 0.3$ for a wall of thickness 1 mm or more and convective heating.

According to Fig. 4, the maximum scatter of the experimental data with respect to the approximating dependences (9) and (10) obtained taking Eq. (11) into account does not exceed ±25%.

Equations (9)-(11) may be recommended for calculations of the heat transfer on boiling in conditions of channel formation ($\tilde{H} \geq \tilde{H}_{lim}$) for water, aqueous solutions, ethanol, and thermodynamically similar liquids at heating surfaces in a disperse layer of particles $\tilde{d}_p \leq 2$ with $\tilde{p} = 1.6 \cdot 10^{-4}$-$1.6 \cdot 10^{-2}$ and $q = 10^3$-$10^5$ W/m$^2$.

In [18], model concepts and calculational dependences for heat transfer based on earlier experimental data [2-4] were proposed. It is of interest to consider the correctness of the model concepts and dependences of [18] on the basis of the whole wealth of experimental data underlying Eqs. (9)-(11). The concepts of [18] coincide in part with the assumptions of [4, 5] considered in the present work. The basic features of the model in [18] are that boiling at a horizontal slit of width s and length b is taken as an analog of boiling in a layer at a wall, and that the rate of onset of particle-layer fluidization is taken as one of the basic parameters. It is incorrect to use these assumptions in the given case ($H > H_{lim}$), since it leads to considerable qualitative and quantitative discrepancy between the calculational dependence of [18] and the experimental data of the present work. For example, in the given case the release of vapor generated at the horizontal surface through the granular layer (in contrast to a slit system) may occur with equal probability from any point of the heating surface. Therefore, the dimensions of the heating surface may not appear in a number of significant parameters, which is confirmed by experiment. In [18], also, it was concluded that $q \sim b$ and $H_{lim} = (2\text{-}3)b$, where b is the plate width or the tube diameter. Experiment indicates that q and $H_{lim}$ are independent of b, and that $H_{lim}$ depends significantly on the physical properties of the liquid. The calculational dependence of [18] was constructed on the basis of the data of [2-4] for the case $H > H_{lim}$. It was shown above that for these conditions d (s in [18]) is a complex function of $d_p$, which corresponds to the presence of an extremum on Fig. 2. In [18], $s(d) \sim d_p$ was assumed without justification for the entire region of Fig. 2, and for qualitative agreement with experiment (Fig. 2), the rate of onset of fluidization was artificially introduced. However, experiment indicates that the motion of components of the system with $H \geq H_{lim}$ (Table 2) is absolutely dissimilar in form to fluidization in the filtration of liquid through the layer. In [18] it was also asserted that in boiling

at a horizontal tube bundle, q depends on b, and no account is taken of the influence on q of the geometry of the bundle and the apparatus, and the layer height, the effect of which on the heat transfer is significant [5, 19]. The calculational dependence of [18] also disagrees with experimental data on the influence of the heating-surface characteristics on the heat transfer, approximated by Eq. (11).

Attempts to calculate heat transfer from the dependence of [18] and comparison with direct experimental data show that the discrepancy amounts to a factor of $10^3$. By introducing correction factors into the calculation (assuming, e.g., that nonsystem units, kJ, have been used instead of J in [18]), the calculation can be made to agree with experiment in order of magnitude, but even in this case the discrepancy reaches a factor of 3-5. Thus, in contrast to Eqs. (9)-(11), the calculational dependences introduced in [18] are neither qualitatively nor quantitatively in agreement with known experimental data.

## NOTATION

| | |
|---|---|
| $c$ | is the specific heat; |
| $d, l$ | are the linear dimensions; |
| $d_p$ | is the mean particle dimension; |
| $H$ | is the particle-layer height; |
| $m$ | is the porosity; |
| $p$ | is the pressure; |
| $q$ | is the heat-flux density; |
| $q^*$ | see Fig. 1; |
| $r$ | is the specific heat of vaporization; |
| $s_{dp}$ | is the mean-square deviation of fraction-particle diameters from $d_p$; |
| $T$ | is the temperature; |
| $w''$ | is the reduced vapor velocity; $\tilde{p} \equiv p/p_{cr}$; $\tilde{d}_p \equiv d_p\sqrt{\sigma/g\rho_L}$; $\tilde{H} = H\sqrt{\sigma/g\rho_L}$; |
| $\alpha$ | is the heat-transfer coefficient; |
| $\delta$ | is the thickness; |
| $\varepsilon \equiv \sqrt{\lambda c\rho}$ | is the heat-assimilation coefficient; |
| $\lambda$ | is the thermal conductivity; |
| $\nu$ | is the kinematic viscosity; |
| $\rho$ | is the density; |
| $\sigma$ | is the surface tension; |
| $\tau$ | is the time; $\tilde{\varepsilon}_w \equiv \varepsilon_w/\varepsilon_{wKh18N10}$; |
| $N_M$ | is the number of given conditions of motion. |

### Subscripts

| | |
|---|---|
| h.d | is the hydrodynamic depression; |
| L | is the liquid; |
| c.d | is the concentrational depression; |
| conv | convective; |
| cr | critical; |
| lim | limiting; |
| s | saturated; |
| v | vapor; |
| w | is the heating wall; |
| p | is the particle material; |
| ef | effective. |

A bar above a symbol denotes the mean.

## LITERATURE CITED


1. Z. R. Gorbis, M. I. Berman, and L. M. Belyi, Inventor's Certificate No. 449227, Byull. Izobret., No. 41 (1974).
2. Z. R. Gorbis and M. I. Berman, Inzh.-Fiz. Zh., 27, No. 3 (1974).

3. M. I. Berman and Z. R. Gorbis, Teploenergetika, No. 11 (1973).
4. Z. R. Gorbis and M. I. Berman, in: Heat and Mass Transfer V [in Russian], Vol. 3, Minsk (1976).
5. M. I. Berman, Author's Abstract of Candidate's Dissertation, FTINT Akad. Nauk Ukr. SSR, Kharkov (1976).
6. D. A. Labuntsov, Teploenergetika, No. 9 (1972).
7. D. N. Sorokin, Author's Abstract of Doctoral Dissertation, MIFI, Moscow (1974).
8. V. A. Grigor'ev et al., Tr. Mosk. Eng. Inst., No. 141 (1972); No. 200 (1974); No. 268 (1975).
9. V. G. Levich, Physicochemical Hydrodynamics, Prentice-Hall (1962).
10. Y. Katto and M. Shoji, Int. J. Heat Mass Transfer, 13, 1299 (1970).
11. H. J. Ouwerkerk, Int. J. Heat Mass Transfer, 14, 1415 (1971).
12. D. A. Labuntsov, Izv. Akad. Nauk SSSR, Otd. Tekh. Nauk, Energ. Transport, No. 1 (1963).
13. Marto and Rosenau, Proc. Am. Soc. Mech. Eng., Ser. C, Heat Transfer, 88, No. 2 (1966).
14. Shurki and Dzhed, Proc. Am. Soc. Mech. Eng., Ser. C, Heat Transfer, 97, No. 1 (1975).
15. V. M. Borishanskii, in: Heat and Mass Transfer [in Russian], Vol. 10, Part 1, Minsk (1973).
16. Ferrell and Ollivitch, in: Heat Tubes [Russian translation], Mir, Moscow (1972).
17. V. A. Grigor'ev, Yu. M. Pavlov, and E. V. Ametistov, in: Heat Transfer 1974. Soviet Research [in Russian], Nauka, Moscow (1975).
18. G. F. Smirnov, Inzh.-Fiz. Zh., 34, No. 5 (1978).
19. M. I. Berman, Z. R. Gorbis, and V. I. Aleksandrov, Inzh.-Fiz. Zh., 36, No. 2 (1979).

# MASS TRANSFER IN A HORIZONTAL GAS – LIQUID FLOW

P. M. Krokovnyi, O. N. Kashinskii, and A. P. Burdukov

UDC 532.529.5

A method and results are presented for local mass transfer from a wall to a two-phase gas-liquid flow; electrochemical techniques are used.

Much research is currently being done on two-phase flows, mainly to provide a detailed description of the turbulent-transport processes and to provide an adequate physical model, which can ensure the development of better methods of calculating two-phase systems. This research on purely hydrodynamic characteristics such as the velocity distribution or the local gas content should be accompanied by research on the turbulent heat and mass transport, in view of its considerable interest. An important aspect is the analogy between the transport of momentum, heat, and mass in a two-phase flow. The rather scanty data on heat transfer in two-phase flows [1-7] are largely incomparable (see, e.g., [7]).

A detailed study has been made [8, 9] of the frictional stress at the wall in a horizontal two-phase gas–liquid flow; we have examined the behavior of the mass-transfer coefficient under similar conditions at large values of the Schmidt number. An electrochemical method was used [10] with an apparatus described in [8]. The working section was a horizontal tube of internal diameter 19 mm and length 6 m. The reduced velocity of the liquid varied over the range 0.1-4 m/sec, while the same for the gas was 0-110 m/sec.

The mixture was produced in a T-shaped mixer, with the liquid supplied through an annular slot of variable width under various conditions. The following flow conditions were implemented: stratified, bolus, bubble, and dispersed-annular (Table 1).

The working section of Fig. 1a was used to measure the local mass-transfer coefficient; this was a nickel block of length 230 mm with a hole of diameter 19 mm separated into two electrically insulated sections. The smaller section of width 6 mm acted as the cathode, while the larger part, which occupied the rest of the perimeter of the tube, was the anode. The part of the cathode adjoining the anode was insulated with a film of foam plastic of thickness 30-50 μm. The cathode contained local mass-transfer transducers (nickel wire of diameter 2 mm and plates of size 0.2 × 2 mm). These transducers were cemented into holes

Institute of Thermophysics, Siberian Branch, Academy of Sciences of the USSR, Novosibirsk. Translated from Inzhenerno-Fizicheskii Zhurnal, Vol. 38, No. 1, pp. 16-22, January, 1980. Original article submitted September 25, 1978.

0022-0841/80/3801-0009$07.50 